Inflammation, Vol. 45, No. 6, December 2022 (© 2022)
https://doi.org/10.1007/s10753-022-01704-2

ORIGINAL ARTICLE

Effects of Resveratrol on Tight Junction Proteins and the Notch1 Pathway in an HT-29 Cell Model of Inflammation Induced by Lipopolysaccharide

Yihua Luo[1], Xueyan Yu[1], Peizhuang Zhao[1], Jun Huang[1] and Xue Huang[1,2]

Received 27 April 2022; accepted 7 June 2022

Abstract— Ulcerative colitis (UC) is closely associated with disruption of intestinal epithelial tight junction proteins. A variety of studies have confirmed that resveratrol (RSV), a natural polyphenolic compound, has a potential anti-inflammatory effect and can regulate the expression of tight junction proteins. However, the mechanism by which RSV regulates the expression of tight junction proteins in the intestinal epithelium remains unclear. Therefore, we investigated the potential effect of RSV on tight junction proteins in an HT-29 cell model of inflammation induced by lipopolysaccharide (LPS) and explored its mechanism of action. First, the downregulated expression of the tight junction proteins occludin, ZO-1, and claudin-1 in the HT-29 cell model of inflammation induced by LPS was reversed by incubation with RSV, accompanied by a decrease in the expression of tumor necrosis factor α-converting enzyme (TACE). Additionally, the Notch1 pathway was attenuated and the expression of the inflammatory factors IL-6 and TNF-α was decreased by treatment with RSV. Second, after Jagged-1 was used in combination with RSV to reactivate the Notch1 pathway, the protective effects of RSV against the LPS-induced reductions in the expression of the tight junction proteins occludin, ZO-1, and claudin-1 and the decreases in the levels of the inflammatory factors IL-6 and TNF-α were abolished. These results suggest that RSV might regulate the expression of tight junction proteins by attenuating the Notch1 pathway.

KEY WORDS: HT-29; Notch1 pathway; Resveratrol; Tight junction protein; Ulcerative colitis

INTRODUCTION

Ulcerative colitis (UC) is an immune-mediated chronic nonspecific intestinal disease characterized by recurrent abdominal pain and diarrhea with mucus, pus, and blood. In recent years, the incidence of UC has gradually increased globally, and UC is expected to affect 30 million people worldwide by 2025 [1]. However, the pathogenesis of UC is still inconclusive. The current view is that the pathogenesis of UC is closely related to

[1]Department of Gerontology and Gastroenterology, The First Affiliated Hospital of Guangxi Medical University, Nanning, Guangxi 530021, China
[2]To whom correspondence should be addressed at Department of Gerontology and Gastroenterology, The First Affiliated Hospital of Guangxi Medical University, Nanning, Guangxi, 530021, China. Email: hb960305@163.com

abnormal structure and function of the intestinal epithelial barrier and an imbalance in the intestinal microbial population [2]. As the first barrier between the body and the environment, the intestinal epithelial barrier prevents microorganisms in the gut from passing through the intestinal mucosa and entering the body to cause abnormal immune responses. The intestinal epithelial barrier constitutes a mechanical barrier, biological barrier, immune barrier, and chemical barrier. The mechanical barrier function of the intestinal epithelium is maintained by the intestinal mucus layer, intestinal epithelial cells, and tight junction proteins located between intestinal epithelial cells. The tight junction proteins are located at the apical surface of the contacts between adjacent intestinal epithelial cells and seal the intercellular space by uniting and connecting adjacent cells, thus maintaining the structural and functional stability of the intestinal epithelial barrier [3]. Previous studies have confirmed that abnormal expression of tight junction proteins such as occludin, ZO-1, and claudin-1 can lead to damage to the integrity of the intestinal epithelial barrier [4], causing diseases related to intestinal epithelial barrier damage (e.g., UC). Therefore, restoring the expression of tight junction proteins is an effective strategy to treat UC.

The occurrence and development of UC are related to the abnormal activity of various signaling pathways in vivo, of which the Notch1 pathway is a key signaling pathway affecting UC [5, 6]. The Notch1 pathway is a highly conserved pathway involved in a series of processes, such as tissue development and homeostasis maintenance [7]. Previous studies have demonstrated that activation of the Notch1 pathway can increase the expression levels of inflammatory factors such as IL-6 and TNF-α, leading to the occurrence of inflammation [8]. In UC mouse models induced by dextran sulfate sodium, after Notch1 pathway activity was inhibited, the secretion of inflammatory factors such as IL-6 and TNF-α was reduced, the differentiation of intestinal epithelial cell populations was restored, and intestinal mucus secretion was increased, thereby alleviating the damaged intestinal epithelial barrier and ameliorating colonic inflammation in mice [9–11].

Resveratrol (RSV) plays an important role in the regulation of Notch1 pathway activity [12, 13]. RSV is a natural polyphenol compound derived from berries, grapes, and other plants; it has biological effects such as anti-tumor, anti-oxidant, and anti-inflammatory effects [14–16], and has thus become a research focus in the development of new drugs for diseases such as cancer and UC. Previous studies have found that RSV, as a supplemental therapy, can alleviate the symptoms of UC and improve the quality of life of UC patients [17, 18]. In addition, related experimental studies have confirmed that in mice with UC induced by dextran sulfate sodium, RSV can inhibit the secretion of inflammatory factors through the PI3K/Akt/VEGFA pathway and NF-κB pathway, ameliorating intestinal inflammation [19, 20]. RSV can also upregulate the expression of intestinal epithelial tight junction proteins in mice [21]. However, in UC-related studies, whether RSV can regulate Notch1 pathway activity and how RSV regulates the expression of tight junction proteins in intestinal epithelial cells are still unclear.

To elucidate the mechanism by which RSV regulates the expression of tight junction proteins in intestinal epithelial cells, this study aimed to establish an intestinal epithelial cell inflammation model by treating HT-29 cells with LPS in vitro and to explore the mechanism by which RSV regulates tight junction proteins in intestinal epithelial cells.

MATERIALS AND METHODS

Materials

RPMI-1640 medium (cat. no. MA0215) and a CCK-8 kit (cat. MA0218) were purchased from Meilun Biological Company (Suzhou, China). Fetal bovine serum (cat. C04001050) was purchased from Biological Industries (VivaCell, Shanghai, China). Serum-free cell cryopreservation solution (cat. no. C40100) and 0.25% EDTA trypsin digestion solution (cat. C125C1) were purchased from New Saimei Biotechnology Company (Suzhou, China). A penicillin–streptomycin mixture (cat. BL505A) was purchased from Biosharp Company (Shanghai, China). Lipopolysaccharide (LPS; *Escherichia coli* serotype 055: B5, cat. no. L2880) was purchased from Sigma (USA). RSV (cat. no. A4182) was purchased from APE (USA). Jagged-1 (cat. no. P1846A) was purchased from MCE (USA). Antibodies against Notch1 (cat. ab52627), Hes1 (cat. no. ab108937), and claudin-1 (cat. no. ab211737) were purchased from Abcam (UK); antibodies against occludin (cat. #91,131), ZO-1 (cat. no. 8193), and GAPDH were purchased from Cell Signaling Technology (USA). A PrimeScript™ RT Reagent Kit with gDNA Eraser (cat. RR047A) was purchased from Takara Company (Beijing, China). The PCR reagent (cat. No. A6002) was purchased from Promega Biotechnology Company

(Beijing, China). Primer constructs were purchased from ShengGong Biotechnology Company (Shanghai, China). Other reagents were purchased from Solarbio Company (Beijing, China) unless otherwise specified.

Cell Culture and Incubations

HT-29 cells were purchased from the Cell Resource Center, Shanghai Institute of Biochemistry and Cell Biology, Chinese Academy of Sciences and were cultured in RPMI-1640 medium containing 10% fetal bovine serum and 1% penicillin–streptomycin at 37 °C in 5% CO_2, and the cell culture medium was changed every 2 days.

When HT-29 cells reached approximately 70–80% confluence, they were starved overnight in serum-free medium. HT-29 cells were preincubated for 4 h with Jagged-1 (10 μmol/L) to activate the Notch1 pathway. Then, the cells were incubated for 4 h in the absence or presence of RSV (50–100 μmol/L) and subsequently treated with LPS (100 μg/mL) for an additional 24 h.

Cell Viability Assay

The effects of drugs on cell viability were detected by a CCK-8 assay. HT-29 cells were seeded into a 96-well plate at a density of 5×10^3 cells/well, and incubated with different concentrations of LPS (0–100 μg/mL), RSV (0–100 μmol/L), and Jagged-1 (0–10 μmol/L). After 24 h or 48 h of incubation, the cells were washed twice with RPMI-1640 medium, and cell culture medium containing 10% CCK-8 solution was then added to each well and further incubated for 1–2 h. After that, the 96-well plate was placed in a microplate reader to measure the absorbance of the cells at 450 nm.

Western Blot Analysis

After the experiments, HT-29 cells were washed with PBS buffer and then transferred to a sterile centrifuge tube, and we prepared cell lysates with a RIPA high-efficiency lysis buffer: protease inhibitor ratio of 100:1. Based on the number of cells in the centrifuge tube, a suitable volume of cell lysate was added to the cells, and the cells were then placed on ice for 30 min for complete lysis. After the cells were completely lysed, they were centrifuged at 12,000 r/min for 15 min in a low-temperature centrifuge at 4 °C, and the supernatant was collected. The protein concentration was determined with a BCA protein detection kit. After determination of the protein concentration, the appropriate amount of protein loading buffer was added to the proteins, and the proteins were then denatured by incubation in a boiling water bath for 7 min. Equal numbers of proteins from each group were separated by SDS–PAGE, and the proteins were then transferred to PVDF membranes. The PVDF membranes were blocked with TBST solution containing 5% nonfat milk powder at room temperature for 1 h, and the corresponding PVDF membranes were then incubated separately with antibodies against occludin, claudin-1, ZO-1, Notch1, Hes1, and GAPDH overnight at 4 °C. After incubation with specific antibodies, the PVDF membranes were washed three times with TBST buffer for 10 min each. After washing, the PVDF membranes were incubated with anti-rabbit IgG at room temperature for 1 h. After incubation, the PVDF membranes were washed with TBST buffer in the dark 3 times for 10 min each. After washing, Odyssey was used to scan the bands in the images, and ImageJ software was used to analyze the bands to determine protein expression levels.

qRT–PCR

After experiments, cells were washed with PBS. According to the instructions, RNAiso Plus solution, isopropanol, and chloroform were used to extract and purify total RNA from HT-29 cells, and we then subjected the RNA to reverse transcription with a PrimeScript™ RT Reagent Kit. In HT-29 cells, the mRNA expression levels of GAPDH, Notch1, Hes1, occludin, ZO-1, claudin1, TNF-α, TACE, and IL-6 were determined by amplification with GoTaq qPCR Master Mix and a StepOnePlus™ instrument with the thermal cycling parameters: initial denaturation at 95 °C for 10 min, followed by 40 cycles of denaturation at 95 °C for 15 s, and annealing at 60 °C for 1 min. The relative mRNA expression levels of the target genes were calculated by the $2^{-\Delta\Delta CT}$ method. The sequences of the forward and reverse primers are shown below: TACE (F) 5′-AATCTCTGTCTCTGTTTC ACCC-3′, (R) 5′-AAAGGGTTTGATAATGCGAACC-3′; TNF-α (F) 5′-AGTGCCACTTTGGCATTATGAGA-3′, (R) 5′-CTTGTGGCAGCAATTGGAAAC-3′; IL-6 (F) 5′-CACTGGTCTTTTGGAGTTTGAG-3′, (R) 5′-GGA CTTTTGTACTCATCTGCAC-3′; occludin (F) 5′-AGT GCCACTTTGGCATTATGAGA-3′,(R) 5′-CTTGTG GCAGCAATTGGAAAC-3′; claudin-1 (F) 5′-GGG CAGATCCAGTGCAAAG-3′, (R) 5′-GGATGCCAA CCACCATCAAG-3′; ZO-1 (F) 5′-GACCAATAGCTG ATGTTGCCAGAG-3′, (R) 5′-TGCAGGCGAATAATG

CCAGA-3′; Notch1 (F) 5′-TCCACCAGTTTGAATGGT CAAT-3′, (R) 5′-CGCAGAGGGTTGTATTGGTTC-3′; Hes1 (F) 5′-AACACTGATTTTGGATGCTCTG-3′, (R) 5′-CACTGTCATTTCCAGAATGTCC-3′; and GAPDH (F) 5′-GCACCGTCAAGGCTGAGAAC-3′, (R) 5′-TGG TGAAGACGCCAGTGGA-3′.

Transmission Electron Microscopy

After experiments, cells were washed with PBS. A 2.5% glutaraldehyde fixative solution was added to the cells for fixation at room temperature in the dark for 2 min. After fixation, we collected the cells in a sterile centrifuge tube and centrifuged them at 1000 r/min for 2 min. After centrifugation, we discarded the fixative solution and added an appropriate amount of electron microscope fixative. The cells were then fixed for 30 min at room temperature in the dark. After fixation, 1% agarose was heated until liquid and poured into a centrifuge tube containing cells to make a cell-agarose block. Subsequently, 0.1% osmic acid was added to the cell-agarose block to fix the cells again at room temperature in the dark for 2 h. After fixation, the cell-agarose block was placed sequentially into 30%, 50%, 70%, 80%, 95%, 100%, and 100% alcohol solutions for 20 min each at room temperature for dehydration. After dehydration, the cell-agarose block was incubated in a 90% acetone solution three times for 10 min each. Finally, the cell-agarose block was embedded and sliced and was then observed and imaged with a transmission electron microscopy.

Statistical Analysis

All experiments were repeated at least three times, and the data are expressed as the means ± SDs. SPSS 22.0 was used for statistical analysis of experimental data, and GraphPad Prism 9.0 was used to generate statistical graphs. One-way ANOVA and Tukey's post hoc test were used to compare differences between each pair of groups. $P < 0.05$ was considered to indicate a statistically significant difference.

RESULTS

The Effects of the Drugs on Cell Viability

The effects of the drugs on the viability of HT-29 cells are shown in Fig. 1a–c. HT-29 cells were incubated with different concentrations of LPS, RSV, and Jagged-1 for 24 h and 48 h, and the effects of the drugs on the viability of HT-29 cells were detected. The results of the CCK-8 assay showed that after HT-29 cells were incubated with the drugs for 24 h, the cell viability was not affected at the highest concentrations tested (the highest concentrations of LPS, RSV, and Jagged-1 were 100 μg/mL, 100 μmol/L, and 10 μmol/L, respectively). However, after HT-29 cells were incubated with the drugs for 48 h, cell viability was affected to varying degrees. To ensure that the subsequent experimental results were not due to drug-induced cell proliferation or apoptosis, we confirmed that the drugs did not affect the viability of

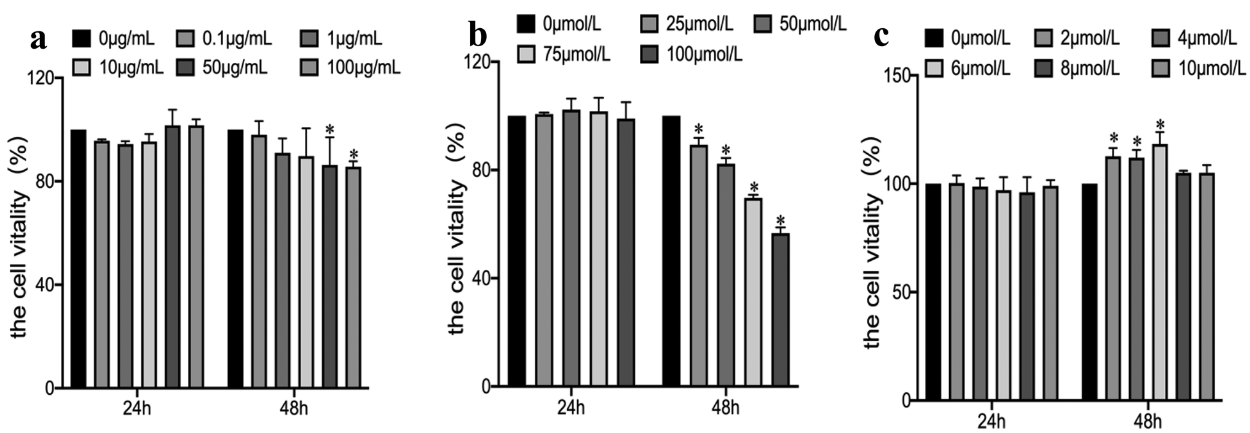

Fig. 1 The effects of the drugs on HT-29 cell viability. **a–c** Cells were incubated with different concentrations of LPS, RSV, and Jagged-1 for 24 h and 48 h, and the effects of the drugs on the viability of HT-29 cells were detected by a CCK-8 assay. The values shown are the means ± SDs; *$P < 0.05$ vs. the control group.

HT-29 cells when used at the selected concentrations and treatment times.

LPS Downregulates the Expression of Tight Junction Proteins in the HT-29 Cell Inflammation Model

LPS can reduce the expression of tight junction proteins; thus, we determined the expression levels of the tight junction proteins occludin, ZO-1, and claudin-1 by Western blotting and qRT-PCR after HT-29 cells were exposed to different concentrations of LPS (0–100 μg/mL) for 24 h. The results are shown in Fig. 2a–g. When the concentration of LPS was 100 μg/mL, it downregulated the expression of occludin, ZO-1, and claudin-1. Therefore, the concentration of LPS used in subsequent experiments was 100 μg/mL.

RSV Downregulates TACE Expression in the HT-29 Cell Inflammation Model

The activation of IL-6 and TNF-α is regulated by TACE. Therefore, we detected the downregulation effect of RSV on LPS-induced TACE expression in the HT-29 cell inflammation model by qRT–PCR, and the results are shown in Fig. 3. An increased level of TACE compared to that in control cells was observed after 24 h of incubation with LPS. RSV prevented this increase in a dose-dependent manner in the HT-29 cell inflammation model, suggesting that RSV can decrease the expression of TACE.

RSV Downregulates the Expression of IL-6 and TNF-α in the HT-29 Cell Inflammation Model

The inflammatory factors IL-6 and TNF-α are important indicators for judging the degree of cellular inflammation. Therefore, we detected the downregulation effect of RSV on LPS-induced IL-6 and TNF-α expression in the HT-29 cell inflammation model by qRT–PCR. The results are shown in Fig. 4a, b. LPS treatment increased the expression levels of the inflammatory factors IL-6 and TNF-α in HT-29 cells compared to the control cells. After HT-29 cells were incubated with RSV, the expression levels of the inflammatory factors IL-6 and TNF-α in the HT-29 cell inflammation model were significantly decreased. These results indicated that RSV has a good anti-inflammatory effect.

RSV Upregulates the Expression of Tight Junction Proteins in the HT-29 Cell Inflammation Model

Occludin, ZO-1, and claudin-1 are important tight junction proteins, which are involved in the maintenance of intestinal epithelial barrier structure and function. Therefore, we detected the expression of occludin, ZO-1, and claudin-1 by Western blot and qRT–PCR. The results are shown in Fig. 5a–g. LPS downregulated the expression of the tight junction proteins occludin, ZO-1, and claudin-1 compared to that in control cells. In contrast, the expression of occludin, ZO-1, and claudin-1 in the HT-29 cell inflammation model was upregulated after incubation with RSV.

We further observed the tight junction structure by transmission electron microscopy. The results are shown in Fig. 6. The normal tight junction structure between HT-29 cells was visualized as narrow and continuous bands by transmission electron microscopy. After HT-29 cells were incubated with LPS, the tight junction structure was loosened, the intercellular space was widened, and the continuity of the bands in the structure was interrupted. Under treatment with RSV, the tight junction structure in the HT-29 cell inflammation model became more tightly connected, the intercellular spaces were narrowed, and the disruption of tight junctions was ameliorated.

Together, these results suggest that RSV can upregulate tight junction proteins to protect the structural integrity of tight junctions.

RSV Attenuated the Activity of the Notch1 Pathway in the HT-29 Cell Inflammation Model

The Notch1 pathway is involved in the transduction of cell differentiation, apoptosis, and survival signaling and plays an important role in the maintenance of intestinal epithelial barrier structure and function. Therefore, we detected the expression of Notch1 pathway-related indicators by Western blot and qRT–PCR. The results are shown in Fig. 7a–e. LPS led to activation of the Notch1 pathway, which was attenuated by RSV in a dose-dependent manner.

RSV Upregulates the Expression of Tight Junction Proteins in the HT-29 Cell Inflammation Model by Attenuating Notch1 Pathway Activity

To verify the mechanism by which RSV regulates the expression of tight junction proteins in the HT-29 cell

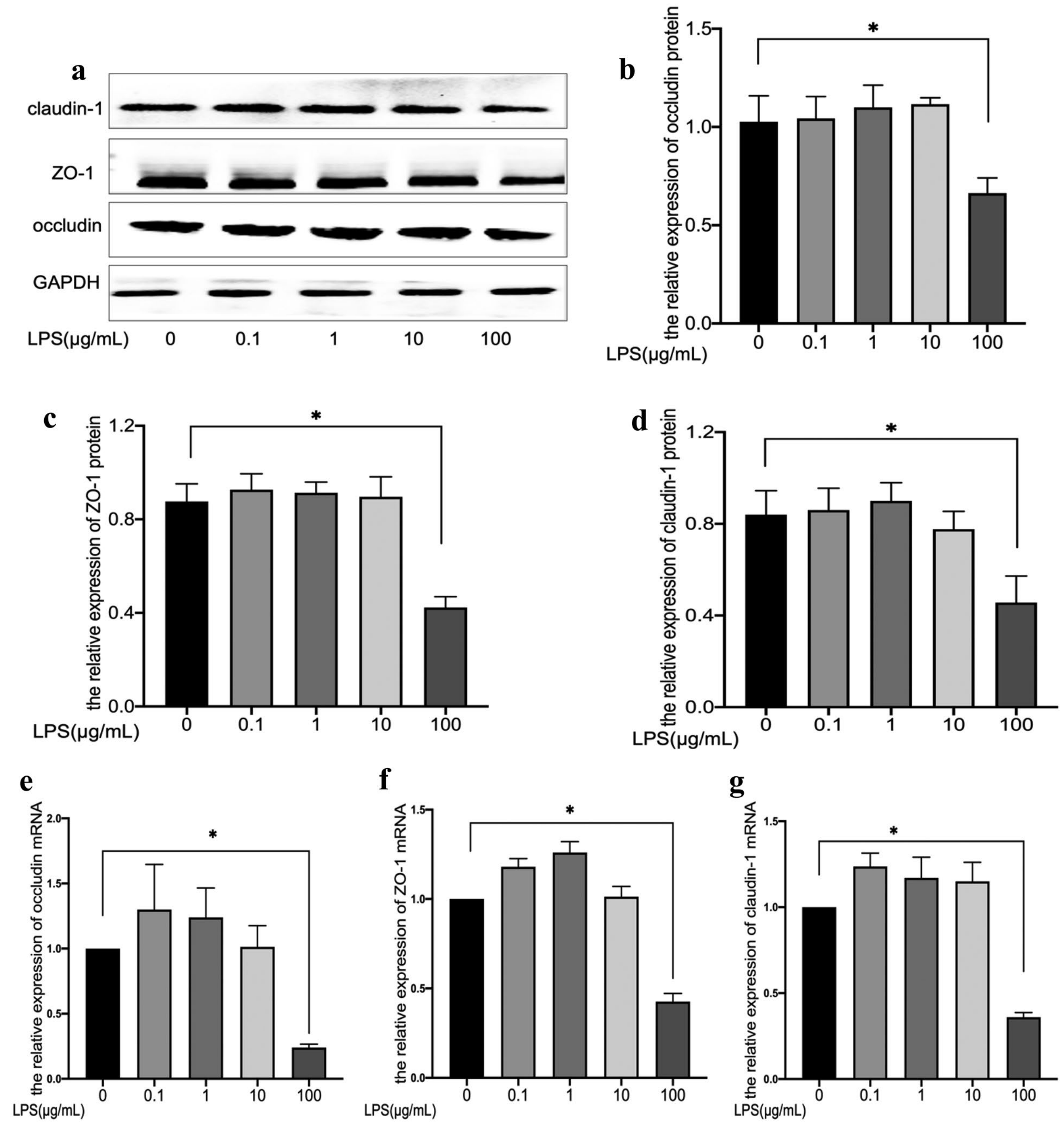

Fig. 2 The effects of LPS on tight junction proteins in the HT-29 cell inflammation model. **a–d** The protein levels of occludin, ZO-1, and claudin-1 were determined by Western blot analysis. **e–g** The mRNA expression levels of occludin, ZO-1, and claudin-1 were determined by qRT–PCR. The values shown are the means ± SDs; *$P < 0.05$.

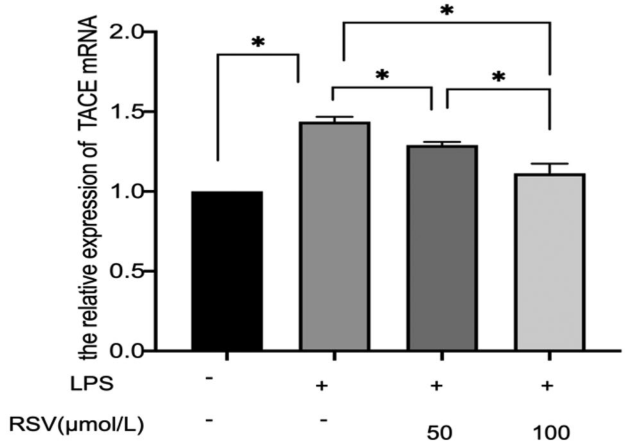

Fig. 3 The effect of RSV on TACE in the HT-29 cell inflammation model. The expression level of TACE was determined by qRT–PCR. The values shown are the means ± SDs; $*P < 0.05$.

inflammation model, we treated the cells with the Notch1 pathway activator Jagged-1. The results are shown in Fig. 8a–e. Jagged-1 abolished the attenuated effect of RSV on LPS-induced activation of the Notch1 pathway.

After Jagged-1 abolished the attenuated effect of RSV on LPS-induced activation of the Notch1 pathway, we detected the expression of the tight junction proteins occludin, ZO-1, and claudin-1 in the HT-29 cell inflammation model after RSV treatment via Western blot and qRT–PCR. The results are shown in Fig. 9a–g. Compared to those in cells incubated with RSV, the expression levels of the tight junction proteins occludin, ZO-1, and claudin-1 in the HT-29 cell inflammation model incubated with both RSV and Jagged-1 were decreased.

We further observed the tight junction structure by transmission electron microscopy, and the results are shown in Fig. 10. Compared to that in cells incubated with RSV, the tight junction structure of cells incubated with both RSV and Jagged-1 was loose, and the intercellular spaces b were widened.

Collectively, these results supported the hypothesis that RSV can upregulate the expression of tight junction proteins by attenuating the activity of the Notch1 pathway.

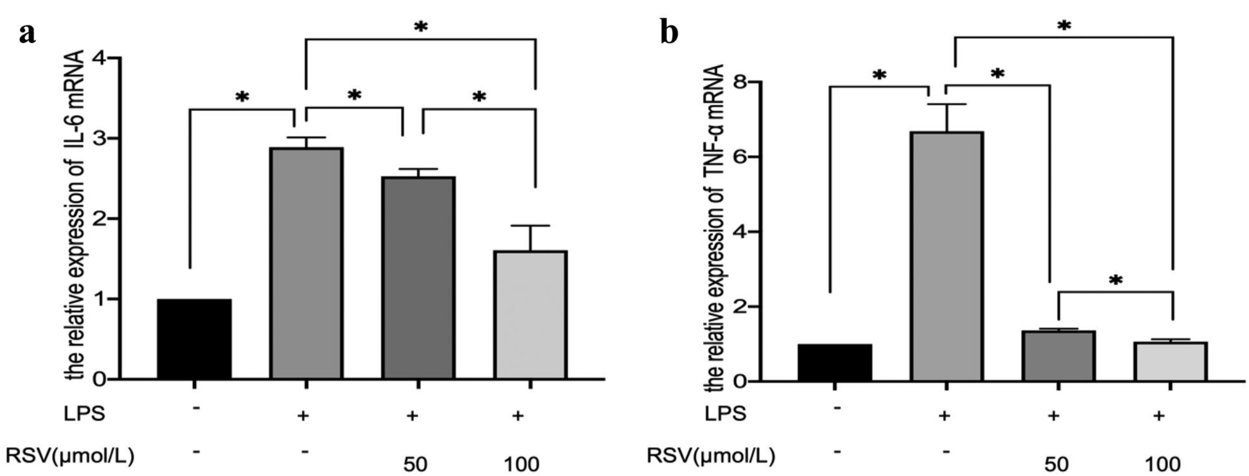

Fig. 4 The effect of RSV on the inflammatory factors IL-6 and TNF-α in the HT-29 cell inflammation model. The expression levels of the inflammatory factors IL-6 and TNF-α in the HT-29 cell inflammation model were determined by qRT–PCR. The values shown are the means ± SDs; $*P < 0.05$.

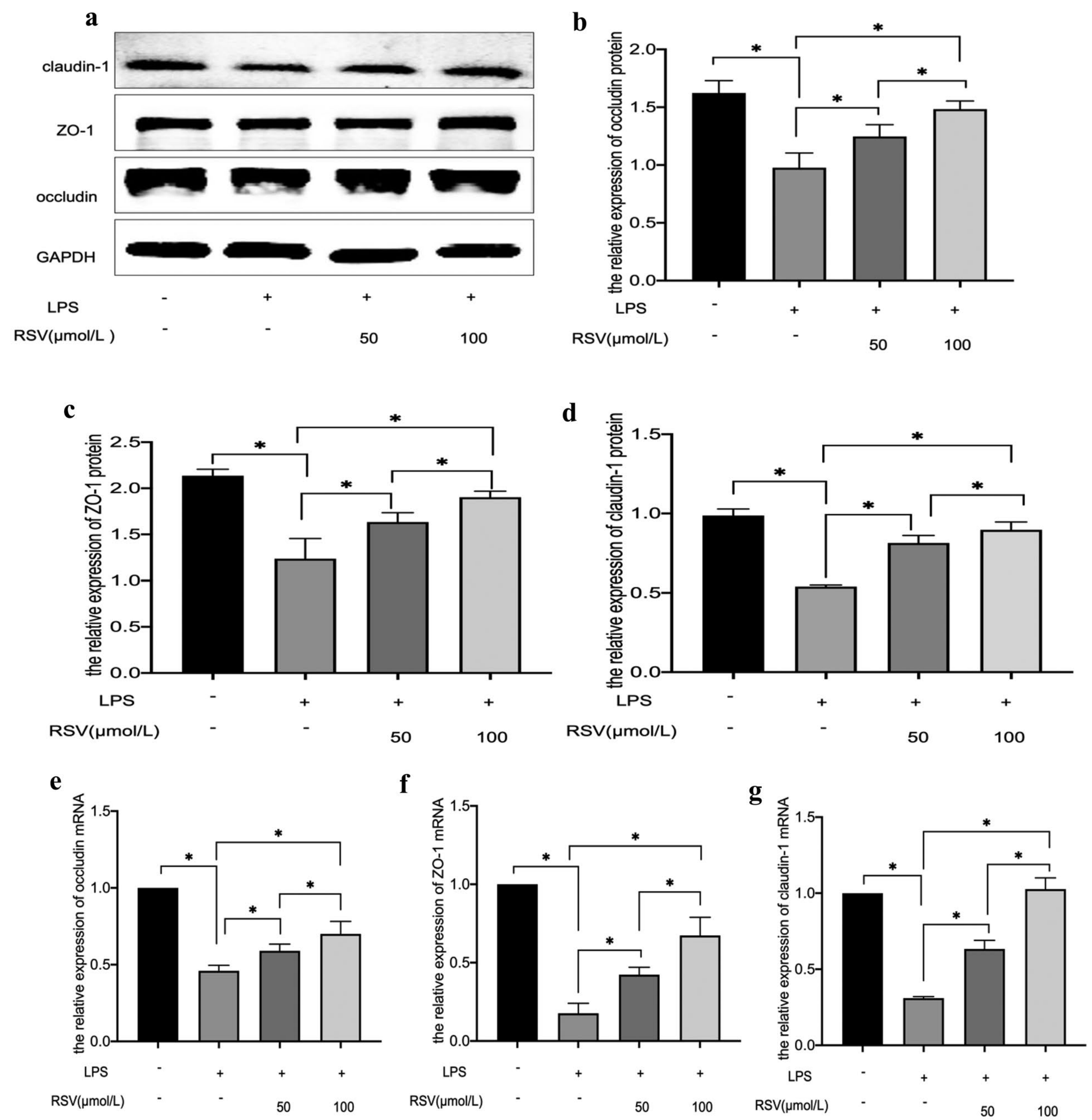

Fig. 5 The effects of RSV on tight junction proteins in the HT-29 cell inflammation model. **a–d** The protein expression levels of occludin, ZO-1, and claudin-1 in the HT-29 cell inflammation model were determined by Western blot analysis. **e–g** The mRNA expression levels of occludin, ZO-1, and claudin-1 in the HT-29 cell inflammation model were determined by qRT–PCR. The values shown are the means ± SDs; *$P < 0.05$.

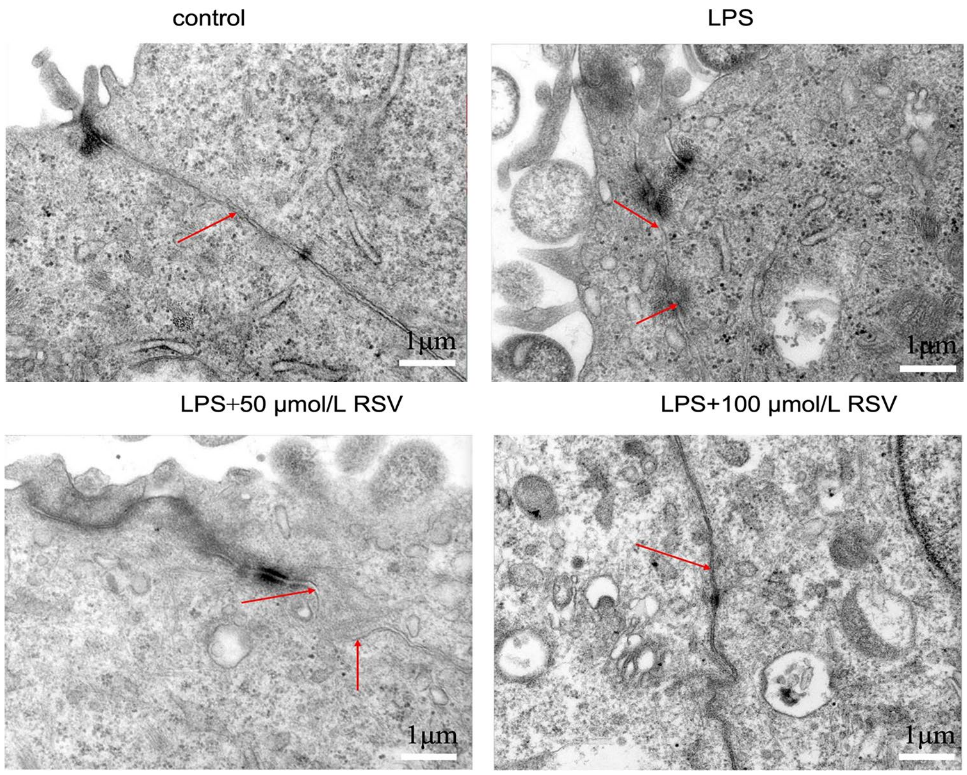

Fig. 6 The effect of RSV on the tight junction structure in the HT-29 cell inflammation model. The structure of tight junctions between cells in the HT-29 cell inflammation model was observed by transmission electron microscopy, and the tight junction structure is indicated by the arrow (scale bar = 1 µm).

Activation of the Notch1 Pathway Promotes the Expression of TACE in the RSV-Treated HT-29 Cell Inflammation Model

The mRNA expression level of TACE in the RSV-treated HT-29 cell inflammation model was determined by qRT–PCR after the Notch1 pathway was activated by Jagged-1. The results are shown in Fig. 11. Compared to that in cells incubated with RSV, the expression level of TACE in the HT-29 cell inflammation model incubated with both RSV and Jagged-1 was increased.

Activation of the Notch1 Pathway Promotes the Expression of IL-6 and TNF-α in the RSV-Treated HT-29 Cell Inflammation Model

The expression of the inflammatory factors IL-6 and TNF-α in the RSV-treated HT-29 cell inflammation model was detected by qRT–PCR after the Notch1 pathway was activated by Jagged-1. The results are shown in Fig. 12a, b. Compared to those in cells incubated with RSV, the expression levels of IL-6 and TNF-α in the HT-29 cell inflammation model incubated with both RSV and Jagged-1 were increased.

DISCUSSION

In the intestine, downregulation of tight junction proteins can lead to impaired intestinal barrier defense, which in turn promotes the occurrence and development of UC [22–24]. Therefore, restoring the expression of tight junction proteins can effectively relieve the symptoms of UC. RSV plays an important role in modulating intestinal inflammation in UC, given that RSV contributes to preserving tight junction protein expression [21, 25], but the mechanism by which RSV regulates the expression of tight junction proteins remains unclear. Therefore,

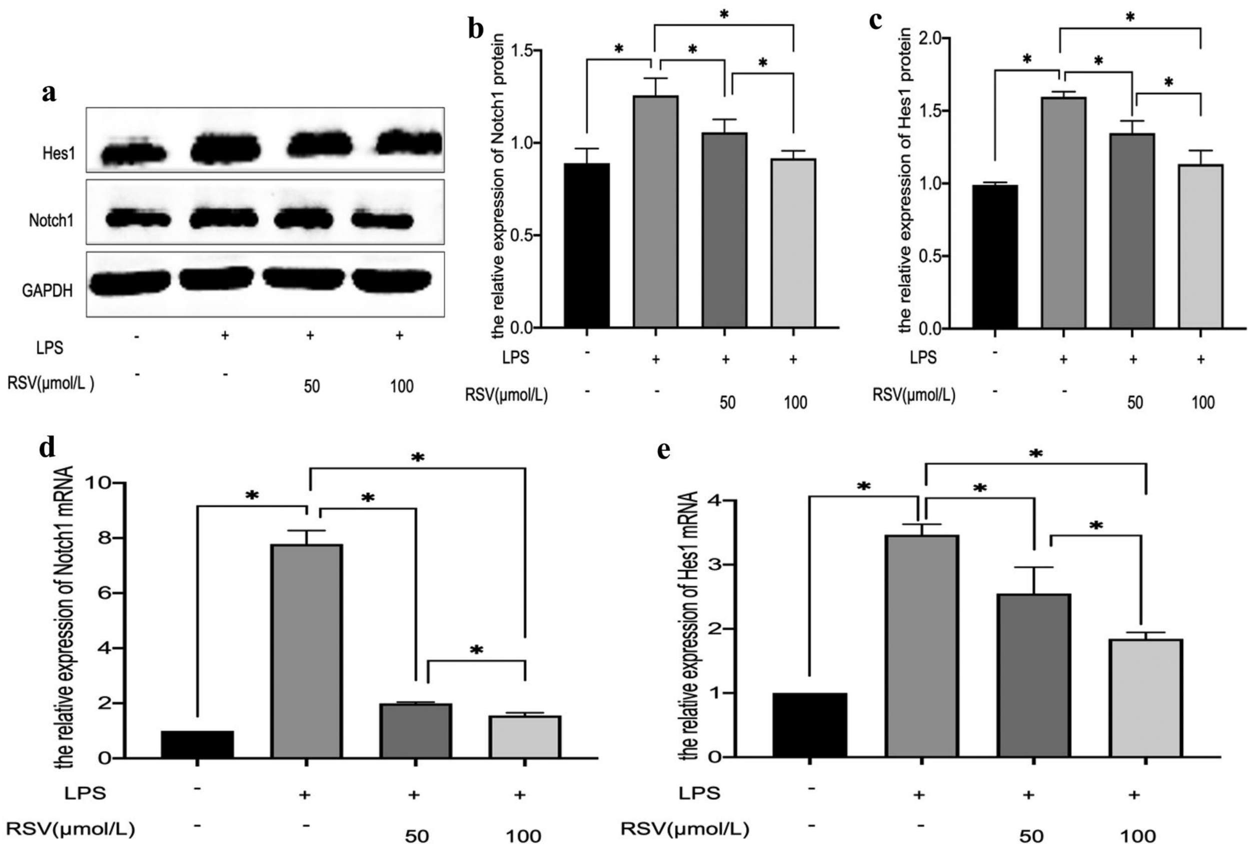

Fig. 7 The effect of RSV on the activity of the Notch1 pathway in the HT-29 cell inflammation model. **a–c** The protein expression levels of Notch1 and Hes1 in the HT-29 cell inflammation model were determined by Western blot analysis. **d** and **e** The mRNA expression levels of Notch1 and Hes1 in the HT-29 cell inflammation model were determined by qRT–PCR. The values shown are the means ± SDs; $*P<0.05$.

this work aimed to explore the potential action mechanism of RSV in the expression of tight junction proteins.

In this study, we found that LPS triggered an increase in TACE, IL-6, and TNF-α expression in HT-29 cells. Additionally, exposure to LPS led to activation of the Notch1 pathway and to a decrease in tight junction protein expression in HT-29 cells. Accordingly, LPS caused disruption of tight junction structure, manifested as widening of the intercellular spaces, and disruption of tight junction continuity, suggesting that the structure of the intestinal epithelial barrier was damaged. These results were consistent with the findings that the expression levels of inflammatory factors and TACE, as well as the activity of the Notch1 pathway, are increased and the expression levels of tight junction proteins are decreased in UC patients [5, 26, 27], indicating that the HT-29 intestinal epithelial cell model of LPS-induced inflammation was successfully established. In addition, all effects of LPS were attenuated by RSV, suggesting that RSV can downregulate the activation of the Notch1 pathway, alleviate cellular inflammation, and upregulate the expression of tight junction proteins in the intestinal epithelium. The findings that RSV can upregulate the expression of tight junction proteins and alleviate inflammation were consistent with those of previous studies in UC models [21, 25]. In subsequent experiments, after the Notch1 pathway activator Jagged-1 was used in combination with RSV in the HT-29 cell inflammation model, the Notch1 pathway was reactivated, and the expression levels of the tight junction proteins occludin, ZO-1, and claudin-1 were decreased. The comprehensive experimental results showed that in the HT-29 cell inflammation model, RSV upregulated the expression of the tight junction proteins

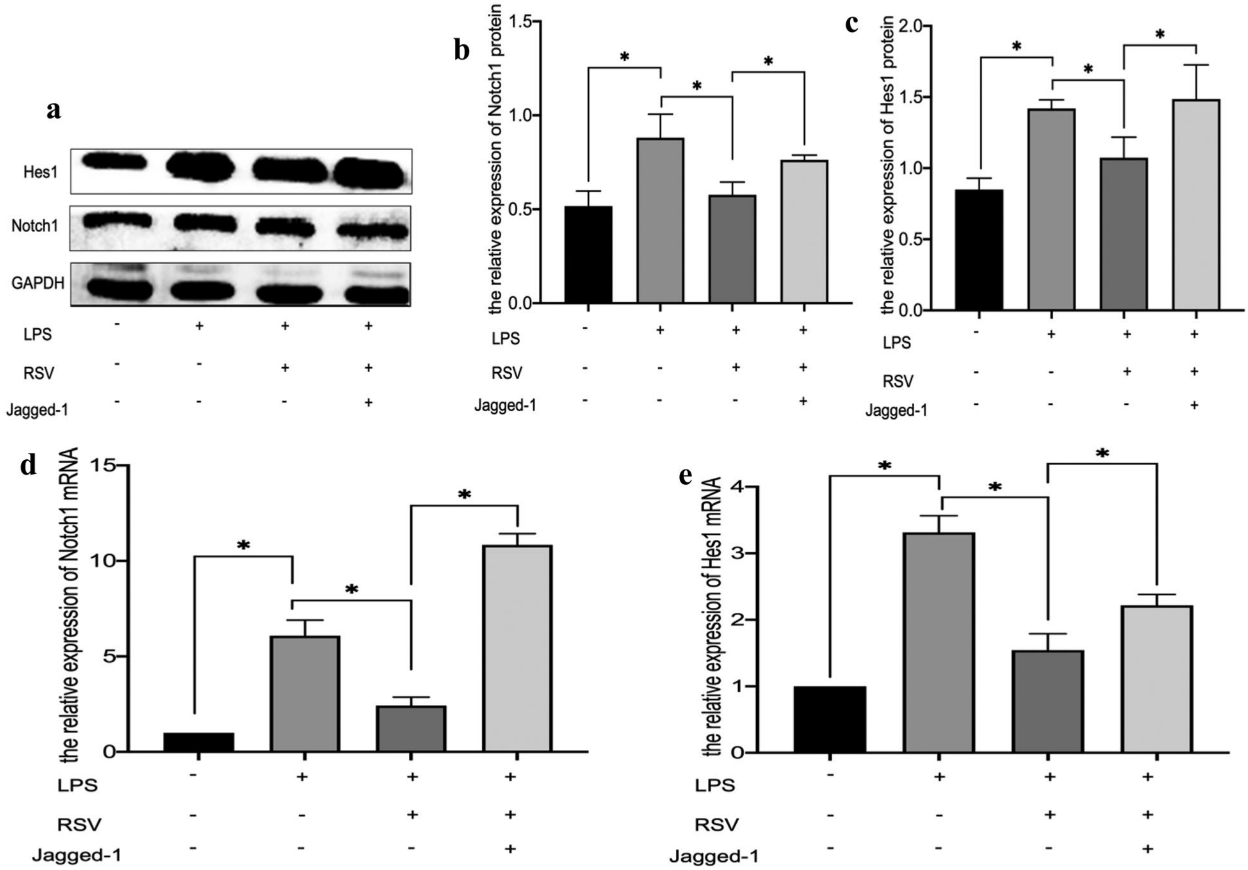

Fig. 8 The effect of Jagged-1 on the activity of the Notch1 pathway in the RSV-treated HT-29 cell inflammation model. **a–c** The protein expression levels of Notch1 and Hes1 in the RSV-treated HT-29 cell inflammation model were determined by Western blot analysis. **d** and **e** The mRNA expression levels of Notch1 and Hes1 in the RSV-treated HT-29 cell inflammation model were determined by qRT–PCR. The values shown are the means ± SDs; **P* < 0.05.

occludin, ZO-1, and claudin-1 via a mechanism related to downregulation of Notch1 pathway activity by RSV.

In this report, we demonstrated that the mechanism by which RSV upregulates the expression of intestinal epithelial tight junction proteins was related to downregulation of Notch1 pathway activation, which was inconsistent with the previous conclusion that "the activation of Notch1 pathway could stabilize the expression of tight junction proteins" [28], and this effect may be related to the decreased expression of the inflammatory factors IL-6 and TNF-α after the Notch1 pathway was inhibited. The Notch1 pathway, as a highly conserved signaling pathway in humans, is mainly composed of Notch1 receptors, Notch1 ligands, and DNA-binding proteins. When ligands and receptors on two adjacent cells interact, the Notch1 pathway is activated in a manner mediated by TACE [29]. After the Notch1 pathway is activated, its ligands can promote the activation of the NF-κB pathway through TRAF6, thereby promoting the secretion of the inflammatory factors IL-6 and TNF-α downstream of the NF-κB pathway [30]. When Notch1 pathway activity is inhibited, the expression levels of the inflammatory cytokines IL-6 and TNF-α are decreased, which in turn alleviates inflammation. In this study, we found that RSV reduced the expression level of TACE and inhibited the activity of the Notch1 pathway in the HT-29 cell inflammation model, which in turn reduced the expression of the inflammatory factors IL-6 and TNF-α and ultimately alleviated detrimental effects on tight junction proteins in intestinal epithelial cells mediated by the inflammatory factors IL-6 and TNF-α. Therefore, when Notch1 pathway activity is properly

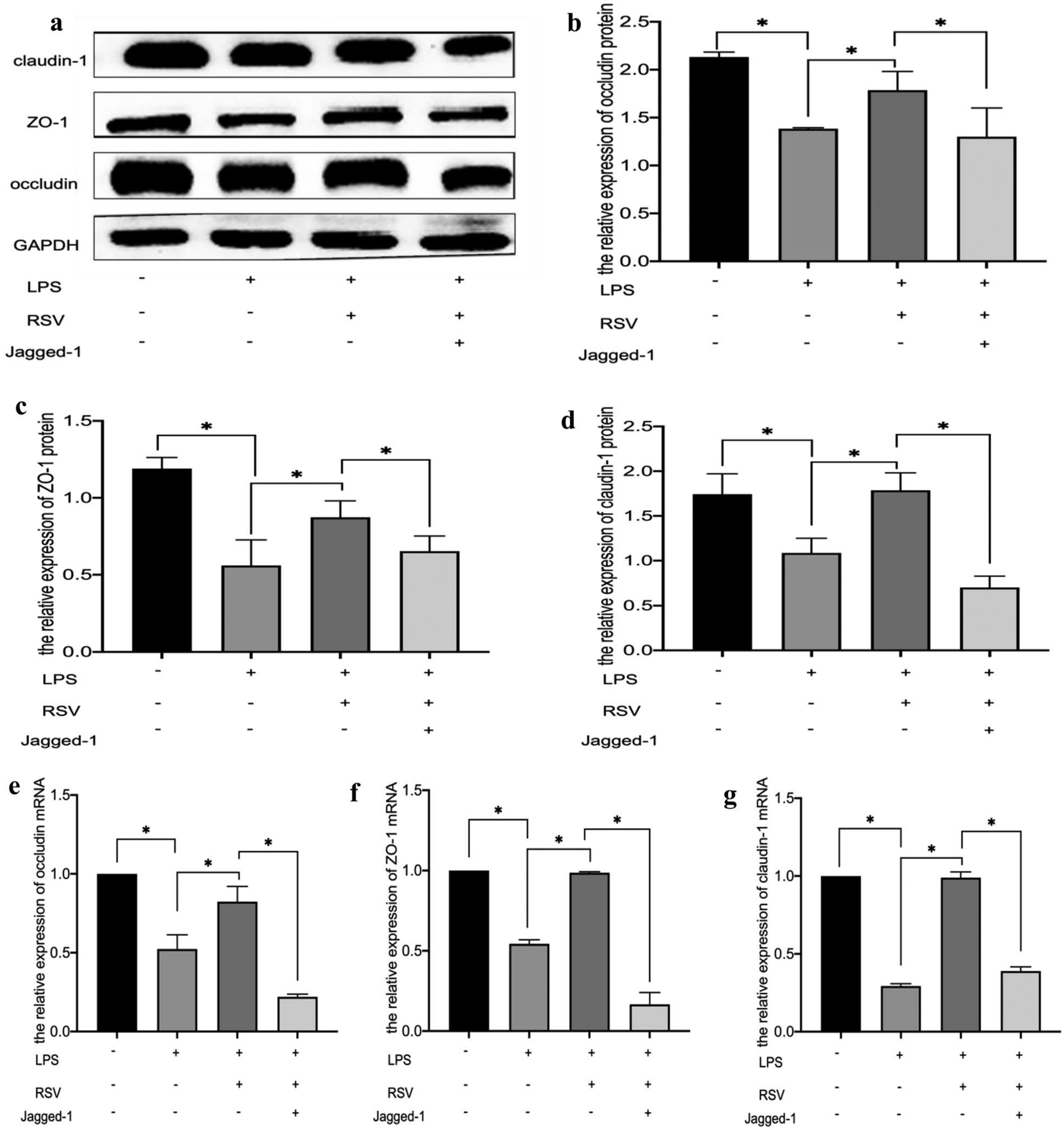

Fig. 9 The effects of Notch1 pathway activation on the expression levels of tight junction proteins in the RSV-treated HT-29 cell inflammation model. **a–d** The protein expression levels of occludin, ZO-1, and claudin-1 in the RSV-treated HT-29 cell inflammation model were determined by Western blot analysis. **e–g** The mRNA expression levels of occludin, ZO-1, and claudin-1 were determined by qRT–PCR in the RSV-treated HT-29 cell inflammation model. The values shown are the means ± SDs; *$P < 0.05$.

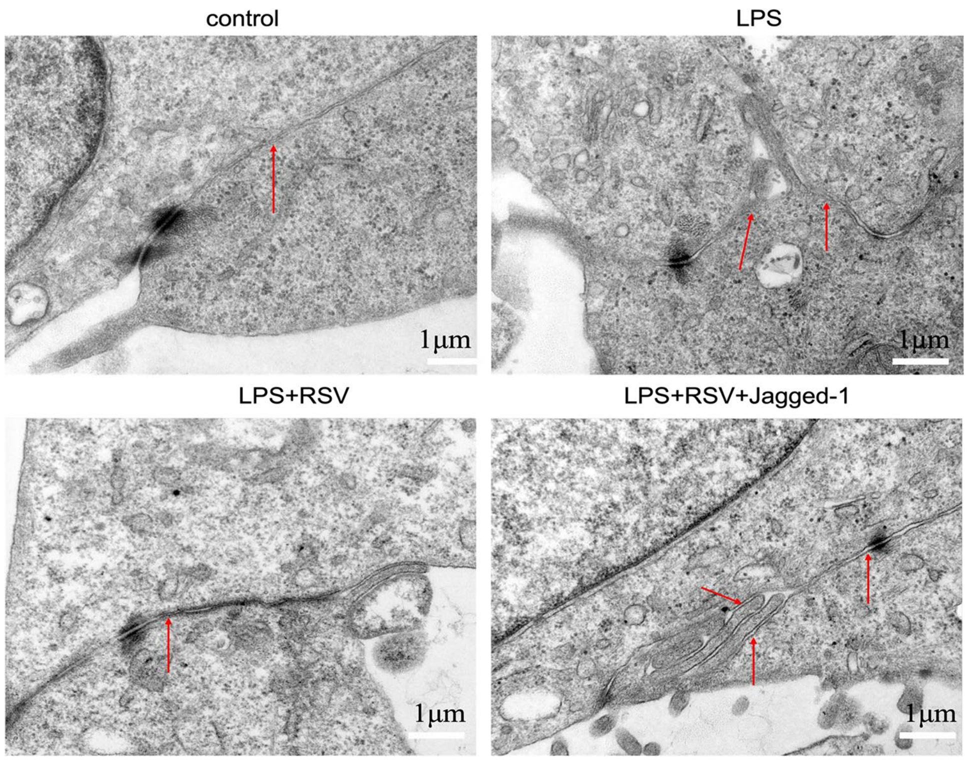

Fig. 10 The effect of Notch1 pathway activation on the tight junction structure in the RSV-treated HT-29 cell inflammation model. The structure of tight junctions between HT-29 cells was observed by transmission electron microscopy, and the tight junction structure is indicated by the arrow (scale bar = 1 μm).

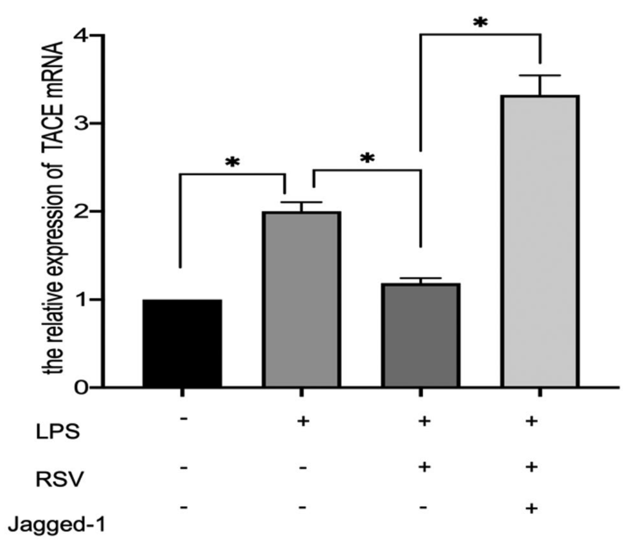

Fig. 11 The effect of Notch1 pathway activation on the expression level of TACE in the RSV-treated HT-29 cell inflammation model. The expression level of TACE in the RSV-treated HT-29 cell inflammation model was determined by qRT–PCR. The values shown are the means ± SDs; $^*P < 0.05$.

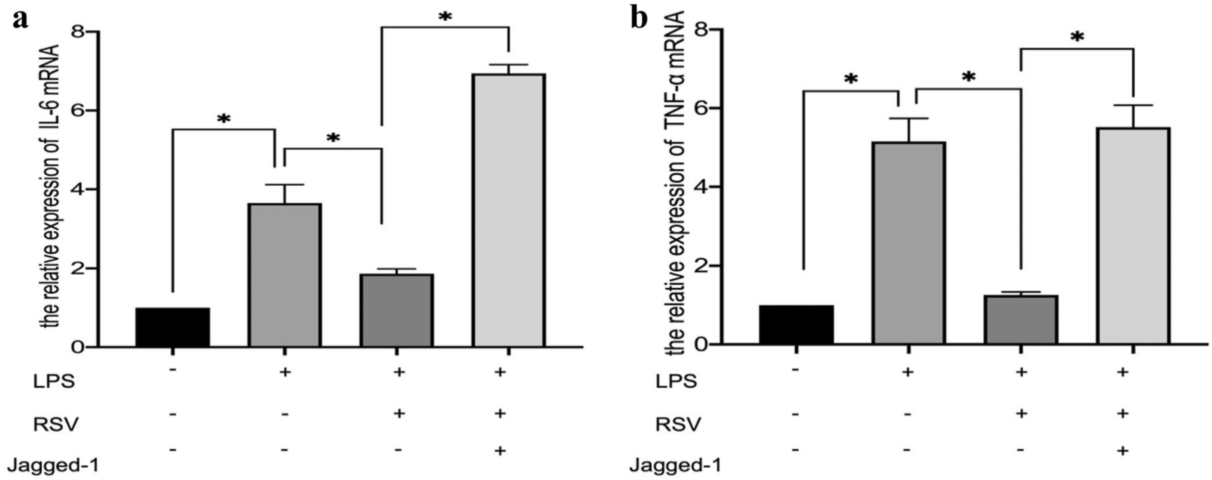

Fig. 12 The effects of Notch1 pathway activation on the expression levels of IL-6 and TNF-α in the RSV-treated HT-29 cell inflammation model. **a** and **b** The expression levels of the inflammatory factors IL-6 and TNF-α in the RSV-treated HT-29 cell inflammation model were determined by qRT–PCR. The values shown are the means ± SDs; $*P < 0.05$.

inhibited, the expression of tight junction proteins is upregulated in the HT-29 cell inflammation model.

Another possible reason for the upregulation of tight junction protein expression after inhibition of the Notch1 pathway is that inhibition of the Notch1 pathway maintains the balance of the intestinal epithelial cell spectrum without affecting the proliferation and renewal of intestinal epithelial cells. The Notch1 pathway plays a dual role in maintaining the stability of intestinal epithelial barrier structure and function. On the one hand, the overactivation of the Notch1 pathway leads to overexpression of the Hes1 gene downstream of the Notch1 pathway, which in turn inhibits the expression of the Math1 gene, resulting in an increase in intestinal absorptive cells and a decrease in secretory cells. Finally, the defense function of the intestinal epithelial barrier is impaired, and the intestinal inflammatory response is aggravated [31]; on the other hand, complete knockout of the Notch1 gene leads to inhibition of intestinal epithelial cell proliferation and renewal in mice, leading to a decrease in the expression of tight junction proteins and thereby aggravating intestinal inflammation [28]. Therefore, proper maintenance of Notch1 pathway activity not only can promote the balance of the intestinal epithelial cell spectrum, but also can ensure the proliferation and renewal of intestinal epithelial cells and maintain intestinal epithelial barrier function. In this study, the activity of the Notch1 pathway was decreased to a certain extent under the action of RSV, and the proliferation and renewal capacity of HT-29 cells were not affected (the results of the CCK-8 assay indicated that RSV had no cytotoxicity in HT-29 cells after 24 h at concentrations ≤ 100 μmol/L), the expressions of tight junction proteins in the intestinal epithelium were upregulated, the intercellular spaces were narrow, and the band continuity was good. As a Notch1 pathway activator, Jagged-1 can alleviate LPS-induced intestinal epithelial cell inflammation by promoting cell proliferation [32]. In this study, the CCK-8 assay and previous experiments showed that when the concentration of Jagged-1 was 10 μmol/L, it did not affect the viability of HT-29 cells and activated the Notch1 pathway. When RSV was combined with Jagged-1, the effect of RSV on upregulating intestinal epithelial tight junction proteins was reversed. By combining the results of this study and previous studies [28], it was concluded that under the premise that the proliferation and renewal of intestinal epithelial cells are unaffected, inhibition of Notch1 pathway activity can upregulate the expression of intestinal epithelial tight junction proteins and alleviate LPS-induced inflammation in HT-29 cells.

In conclusion, this study demonstrated that RSV significantly reduces the LPS-induced inflammatory response and ameliorates detrimental effects on intestinal epithelial tight junction proteins by attenuating the activation of the TACE and Notch1 pathways, suggesting that RSV may be a potentially effective drug for the treatment of UC.

AUTHOR CONTRIBUTION

Xue Huang contributed to the conception of the paper and reviewed the final manuscript. Yihua Luo performed most of the experiments described in the manuscript and wrote the paper. Xueyan Yu performed the data analysis. Peizhuang Zhao and Jun Huang contributed to constructive discussions.

FUNDING

This work was financially supported by a grant from the National Natural Science Foundation of China (81,660,093).

DATA AVAILABILITY

The data that support the findings of this study are available on request from the corresponding author.

DECLARATIONS

Ethical Approval Not applicable.

Consent for Publication All authors have read and approved the submission

Competing Interest The authors declare no competing interests.

REFERENCES

1. Kaplan, G.G. 2015. The global burden of IBD: From 2015 to 2025. *Nature Reviews. Gastroenterology & Hepatology* 1212: 720–727. https://doi.org/10.1038/nrgastro.2015.150.
2. Porter, R.J., R. Kalla, and G.T Ho. 2020. Ulcerative colitis: recent advances in the understanding of disease pathogenesis. *F1000Res* 9. https://doi.org/10.12688/f1000research.20805.1.
3. Schmitz, H., C. Barmeyer, M. Fromm, N. Runkel, H.D. Foss, C.J. Bentzel, E.O. Riecken, and J.R. Dschulzke. 1999. Altered tight junction structure contributes to the impaired epithelial barrier function in ulcerative colitis. *Gastroenterology* 1162: 301–309. https://doi.org/10.1016/s0016-5085(99)70126-5.
4. Chelakkot, C., J. Ghim, and S.H. Ryu. 2018. Mechanisms regulating intestinal barrier integrity and its pathological implications. *Experimental & Molecular Medicine* 508: 1–9. https://doi.org/10.1038/s12276-018-0126-x.
5. Ghorbaninejad, M., R. Heydari, P. Mohammadi, S. Shahrokh, M. Haghazali, B. Khanabadi, and A. Meyfour. 2019. Contribution of NOTCH signaling pathway along with TNF-alpha in the intestinal inflammation of ulcerative colitis. *Gastroenterol Hepatol Bed Bench* 12Suppl1: S80-S86.
6. Gersemann, M., S. Becker, I.K. Bler, M. Koslowski, G. Wang, K.R. Herrlinger, J. Griger, P. Fritz, K. Fellermann, and M. Schwab. 2009. Differences in goblet cell differentiation between Crohn's disease and ulcerative colitis. *Differentiation* 771: 84–94. https://doi.org/10.1016/j.diff.2008.09.008.
7. Gordon, W.R., K.L. Arnett, and S.C. Blacklow. 2008. The molecular logic of Notch signaling—a structural and biochemical perspective. *J Cell Sci* 121Pt 19: 3109–3119. https://doi.org/10.1242/jcs.035683.
8. Wan, Y., and Z.Q. Yang. 2020. LncRNA NEAT1 affects inflammatory response by targeting miR-129–5p and regulating Notch signaling pathway in epilepsy. Cell Cycle 194: 419–431. https://doi.org/10.1080/15384101.2020.1711578.
9. Hui, Y., S.G. Yan, and Q. Wang. 2020. Effects of 6-Shogaol on Notch signaling pathway in colonic epithelial cells of ulcerative colitis mice. *Zhongguo Ying Yong Sheng Li Xue Za Zhi* 361: 90–93. https://doi.org/10.12047/j.cjap.5889.2020.020.
10. Lin, J.C., J.Q. Wu, F. Wang, F.Y. Tang, J. Sun, B. Xu, M. Jiang, Y. Chu, D. Chen, and X. Li. 2019. QingBai decoction regulates intestinal permeability of dextran sulphate sodium-induced colitis through the modulation of notch and NF-kappaB signalling. *Cell Proliferation* 522: e12547. https://doi.org/10.1111/cpr.12547.
11. Zhao, Y., H. Luan, H. Gao, and X. Wu,Y Zhang, and R. Li. 2020. Gegen Qinlian decoction maintains colonic mucosal homeostasis in acute/chronic ulcerative colitis via bidirectionally modulating dysregulated Notch signaling. *Phytomedicine* 68: 153182. https://doi.org/10.1016/j.phymed.2020.153182.
12. Zong, D.D., X.M. Liu, J.H. Li, R.Y. Ouyang, Y.J. Long, P. Chen, and Y. Chen. 2021. Resveratrol attenuates cigarette smoke induced endothelial apoptosis by activating Notch1 signaling mediated autophagy. *Respiratory Research* 221: 22. https://doi.org/10.1186/s12931-021-01620-3.
13. Kim, T.H., J.H. Park, and J.S. WO. 2019. Resveratrol induces cell death through ROS-dependent downregulation of Notch1/PTEN/Akt signaling in ovarian cancer cells. *Molecular Medicine Reports* 194: 3353–3360. https://doi.org/10.3892/mmr.2019.9962.
14. Santos, M.A., F.N. Franco, C.A. Caldeira, G.R.D. Araújo, A. Vieira, and M.M. Chaves. 2021. Antioxidant effect of resveratrol: Change in MAPK cell signaling pathway during the aging process. *Archives of Gerontology and Geriatrics* 92: 104266. https://doi.org/10.1016/j.archger.2020.104266.
15. Zhang, Q., H. Huang, F. Zheng, H. Liu, F. Qiu, Y. Chen, C. Liang, and Z. Dai. 2020. Resveratrol exerts antitumor effects by downregulating CD8(+)CD122(+) Tregs in murine hepatocellular carcinoma. *Oncoimmunology* 91: 1829346. https://doi.org/10.1080/2162402X.2020.1829346.
16. Salla, M., V. Pandya, K.S. Bhullar, E. Kerek, Y.F. Wong, R. Losch, J. Ou, F.S. Aldawsari, C. Velazquez-Martinez, and A. Thiesen. 2020. Resveratrol and resveratrol-aspirin hybrid compounds as potent intestinal anti-inflammatory and anti-tumor drugs. *Molecules* 2517. https://doi.org/10.3390/molecules25173849.
17. Samsamikor, M., N.E. Daryani, P.R. Asl, and H. Azita. 2016. Resveratrol supplementation and oxidative/anti-oxidative status in patients with ulcerative colitis: A randomized, double-blind, placebo-controlled pilot study. *Archives of Medical Research* 474: 304–309. https://doi.org/10.1016/j.arcmed.2016.07.003.
18. Samsamikor, M., N.E. Daryani, P.R. Asl, and H. Azita. 2015. Anti-inflammatory effects of resveratrol in patients with ulcerative colitis: A randomized, double-blind, placebo-controlled pilot study. *Archives of Medical Research* 464: 280–285. https://doi.org/10.1016/j.arcmed.2015.05.005.
19. Zhu, F., J. Zheng, F. Xu, Y. Xi, J. Chen, and X. Xu. 2021. Resveratrol alleviates dextran sulfate sodium-induced acute ulcerative

colitis in mice by mediating PI3K/Akt/VEGFA pathway. *Frontiers in Pharmacology* 12: 693982. https://doi.org/10.3389/fphar.2021.693982.

20. Liu, B., S. Li, X. Sui, L. Guo, X. Liu, H. Li, L. Gao, S. Cai, Y. Li, T. Wang, and X. Piao. 2018. Root extract of *Polygonum cuspidatum* Siebold & Zucc. ameliorates DSS-induced ulcerative colitis by affecting NF-kappaB signaling pathway in a mouse model via synergistic effects of polydatin, resveratrol, and emodin. *Front Pharmacol* 9: 347. https://doi.org/10.3389/fphar.2018.00347.
21. Pan, H.H., X.X. Zhou, Y.Y. Ma, Y.Y. Ma, W.S. Pan, F. Zhao, M.S. Yu, and J.Q. Liu. 2020. Resveratrol alleviates intestinal mucosal barrier dysfunction in dextran sulfate sodium-induced colitis mice by enhancing autophagy. *World Journal of Gastroenterology* 2633: 4945–4959. https://doi.org/10.3748/wjg.v26.i33.4945.
22. Rawat, M., M. Nighot, R. Al-Sadi, Y. Gupta, D. Viszwapriya, G. Yochum, W. Koltun, and T.Y. Ma. 2020. IL1B increases intestinal tight junction permeability by up-regulation of MIR200C-3p, which degrades occludin mRNA. *Gastroenterology* 1594: 1375–1389. https://doi.org/10.1053/j.gastro.2020.06.038.
23. Pochard, C., J. Gonzales, A. Bessard, M.M. Mahe, A. Bourreille, N. Cenac, A. Jarry, E. Coron, J. Podevin, and G. Meurette. 2021. PGI2 inhibits intestinal epithelial permeability and apoptosis to alleviate colitis. *Cellular and Molecular Gastroenterology and Hepatology* 123: 1037–1060. https://doi.org/10.1016/j.jcmgh.2021.05.001.
24. Ma, Y., J. Yue, Y. Zhang, C. Shi, M. Odenwald, W.G. Liang, Q. Wei, A. Goel, X. Gou, and J. Zhang. 2017. ACF7 regulates inflammatory colitis and intestinal wound response by orchestrating tight junction dynamics. *Nature Communications* 8: 15375. https://doi.org/10.1038/ncomms15375.
25. Mayangsari, Y., and T. Suzuki. 2018. Resveratrol ameliorates intestinal barrier defects and inflammation in colitic mice and intestinal cells. *Journal of Agricultural and Food Chemistry* 6648: 12666–12674. https://doi.org/10.1021/acs.jafc.8b04138.
26. Brynskov, J., P. Foegh, G. Pedersen, C. Ellervik, T. Kirkegaard, A. Bingham, and T. Saermark. 2002. Tumour necrosis factor alpha converting enzyme (TACE) activity in the colonic mucosa of patients with inflammatory bowel disease. *Gut* 511: 37–43. https://doi.org/10.1136/gut.51.1.37.
27. Yamamoto-Furusho, J.K., E.J. Mendivil-Rangel, and B.G. Fonseca-Camarillo. 2012. Differential expression of occludin in patients with ulcerative colitis and healthy controls. *Inflammatory Bowel Diseases* 1810: E1999. https://doi.org/10.1002/ibd.22835.
28. Mathern, D., L. Laitman, Z. Hovhannisyan, D. Dunkin, S. Farsio, T. Malik, G. Roda, A. Chitre, A. Iuga, and G. Yeretssian. 2014. Mouse and human Notch-1 regulate mucosal immune responses. *Mucosal Immunology* 74: 995–1005. https://doi.org/10.1038/mi.2013.118.
29. Kopan, R., and M.X.G. Ilagan. 2009. The canonical Notch signaling pathway: Unfolding the activation mechanism. *Cell* 1372: 216–233. https://doi.org/10.1016/j.cell.2009.03.045.
30. Zhang, Q., C. Wang, Z. Liu, X. Liu, C. Han, X. Cao, and N. Li. 2012. Notch signal suppresses Toll-like receptor-triggered inflammatory responses in macrophages by inhibiting extracellular signal-regulated kinase 1/2-mediated nuclear factor kappaB activation. *Journal of Biological Chemistry* 2879: 6208–6217. https://doi.org/10.1074/jbc.M111.310375.
31. Alvarado, D.M., B. Chen, M. Iticovici, A.I. Thaker, N. Dai, K.L. VanDussen, N. Shaikh, C.K. Lim, G.J. Guillemin, P.I. Tarr, and M.A. Ciorba. 2019. Epithelial indoleamine 2,3-dioxygenase 1 modulates aryl hydrocarbon receptor and notch signaling to increase differentiation of secretory cells and alter mucus-associated microbiota. *Gastroenterology* 1574 (1093–1108): e1011. https://doi.org/10.1053/j.gastro.2019.07.013.
32. Cong, Z., G. Ye, Z. Bian, M.H. Yu, and M. Zhong. 2018. Jagged-1 attenuates LPS-induced apoptosis and ROS in rat intestinal epithelial cells. *International Journal of Clinical and Experimental Pathology* 118: 3994–4003.